Moroccan Journal of Chemistry
ISSN: 2351-812X
http://revues.imist.ma/?journal=morjchem&page=login
Monajjemi. / Mor. J. Chem. 6 N°4 (2018) 588-600

Symmetry comparison of BH5 & CH_5^+ ion and deuterated variants of $BH_xD_{(5-x)}$: real or art factual stabilities

M. Monajjemi

Department of Chemical Engineering, Central Tehran Branch, Islamic Azad University, Tehran, Iran

** Corresponding author:*
Maj.monajjemi@iauctb.ac.ir
Received 04 Sept 2017,
Revised 28 Aug 2018,
Accepted 10 Oct 2018

Abstract

In this work, we investigated the symmetry and electronics behavior of BH_5 and CH_5^+ which belong to the D_3h point group of a primary considerationin the ground state. Protonated methane, CH_5^+, has unusual vibrational and rotational behavior due to its three nonequivalent equilibrium structures have nearly identical energies and five protons scramble freely. In this study we calculate the structures of BHxD (5-x) and CHxD (5-x) +using Moller Plesset, single and double excitations (CISD) and CASSCF (8, 9) with an augmented TZ (3d1f1g, 2p1d) basis set. Our study confirms that ground state may in fact belong to the point group C2v or Cs. The normal modes vibration of deuterated variants agrees with mechanism of C-H and B-H bonds which are broken and reformed all time. These studies are confirmed relative stability of CH5+ with respect to methane and the stability of BH_5in comparison with other known boron hydrides

Keywords: *symmetry, BH_5, CH_5^+ ions, deuterated variants of methane*

1. Introduction

Recently studies have predicated a proton affinity for methane approximately around 7 electron volte which much higher than the experimental estimation [1-4]. Protonated methane (CH_5^+) as a carbonation with three-center two-electron bonding has been subject of various theoretical and experimental investigations since its first detection in 1952[1, 5-7].Kreevoy and coworkers exhibited a C_s point group for BH_5 with two bands as A' and A" shifted related to frequencies of 30 and 70 cm^{-1} [8].There are some questions for(H_2+BH_3), combination that are mostly about the effective BH_5 structure[9].Hyper-coordinate carbon chemistry and super-acid [10, 11]is an important key which is highly relevant in plasma chemistry[12, 13]. For decades and even up to now, CH_5^+ has provided some challenges due to the correlated large-amplitude motion of its five protons around the carbon for theoreticians and as well as for experimentalists .Protonated (BH_4^-+H^+) and (CH_4 +H^+) structures with three-center two-electron bonding have been the subject of various theoretical and experimental studies since its first investigation by Micheles and coworkers in 1971[14]. Keiran [15] and coworkers has applied a quantum diffusion Monte-Carlo (QDMC) calculation for estimating the ground-state zero-point energy from an interpolated PES. They exhibited that the zero-point energy (ZPE) as a function of the number by 150 points has converged to within $\pm$0.5 kJ/mol. And also the converged fully an-harmonic ZPE on the interpolated PES calculated 132.72 was significantly lower than the CCSD(T)/aug-cc-pVTZor MP2/cc-pVTZ harmonic zero-point energy of the global minimum structure. For decades and even up to now, although a few works have been studied for CH_5^+, there is no work for BH_5 except a work with Schreiner and coworkers in 1994[16]. In addition, although a few theoretical papers have been published on the quantum mechanics of these systems, a better understanding requires spectral and conformational analysis through deuterated variants which is novel approach in this work. Up to now there is no attempt for comparing the structures of CH_5^+ and deuterated variants BH_5 in view point of rotational and conformational analysis.

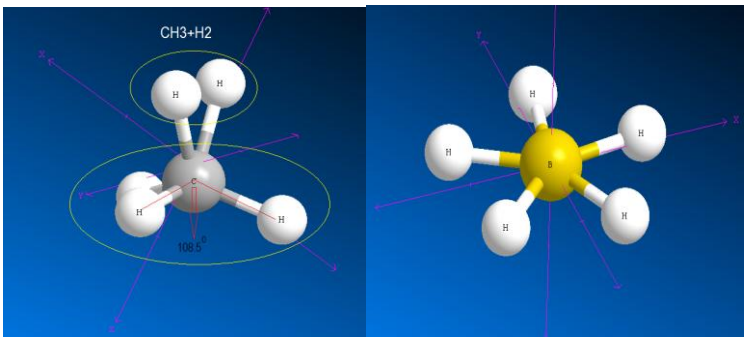

Scheme 1: The optimized position of BH_5 and $CH5^+$ in ground state and low level calculation.

Based on the bimodal character of the H-H radial distribution function, it is obvious that the ground-state of CH_5^+ wave function compare to BH_5 does have global minimum energy configuration *Cs* character; however, there is considerable delocalization of the protons, shows a ground-state structure with symmetrical structure than the *Cs* configuration (scheme1). Both BH_5 and CH_5^+ consist of three configuration including static equilibrium structure of ground state and two transition states, as (1): e-*Cs* (I) isomer consists of a three-center two-electron bond associating two hydrogen and a BH_3 or CH_3 tripod, while H_2 moiety is attached in an eclipsed orientation. (2): A staggered (s-Cs) saddle-point [17], obtained by thirty degree rotation of the H_2 moiety, is barely higher in energy(0.1 kcal mol^{-1}) than the ground state and (3): the third stationary point is a saddle-point [with C_{2V} symmetry that is about $\approx$0.8 kcal mol^{-1} above the e-Cs global minimum structure[17,18]. An approach as a one of the scenarios enables easy exchange of the hydrogen sites which so-called 'hydrogen scrambling [16, 17]. This phenomenon has occurred by isomerization

transitions between different degenerate stats of e-Cs minima through the s-Cs transition and C_{2v} structure [19] (**Fig**.1).

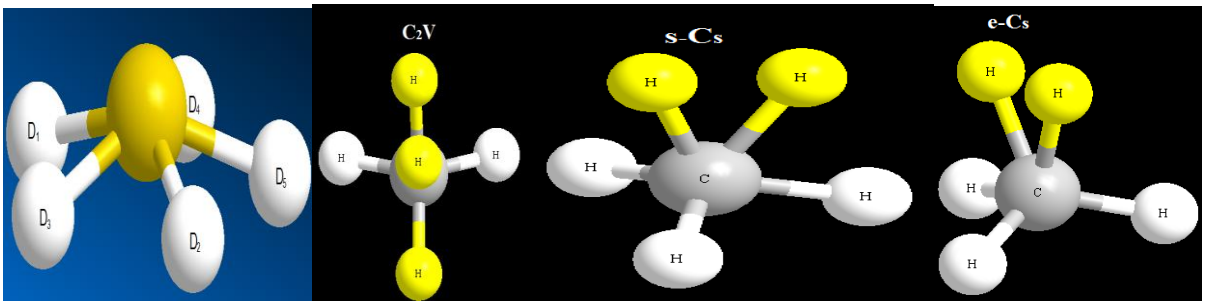

Fig.1: unstable structure of BD5 and e-C_s for global minima structures with CH_3 tripod, staggered saddle point and H_2 moiety

Schreiner et al. [16, 20] exhibited, at room temperature; the borane–hydrogen complex BH5 is unstable toward dissociation by 6.8 kcal mol−1. However, at the absolute zero (0 K), the complex forms exothermically (−1.4 kcal mol−1). The theoretical De value (6.3 kcal mol−1) appears to be effectively converged with respect to basis set and theoretical method [20]. The inclusion of perturbation triple excitations accounts for 36% of the total binding energy, a remarkable effect. Hydrogen scrambling via a C2v structure seems unlikely since the activation barrier for this process is at least 2.8 kcal mol−1 higher than the dissociation barrier of BH5 into BH3 and H2[16, 20] (**Fig**.2).

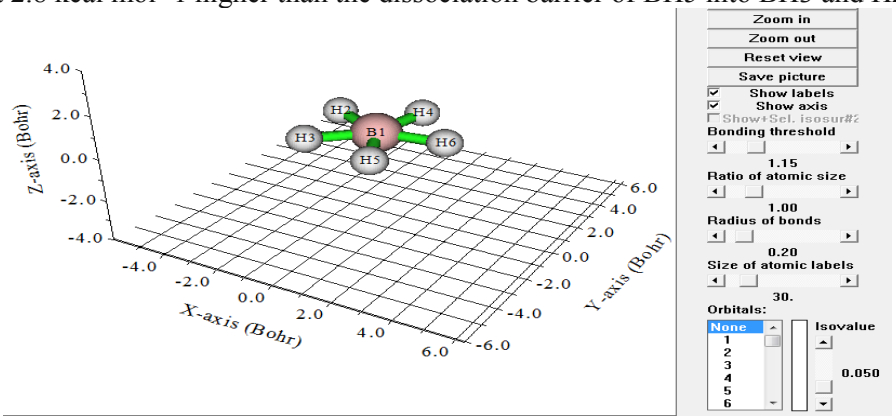

Fig.2: The 3DGeometry of BH5 in ground state.

Generally it might be resulted from the zero point energy on the basis of the harmonic values which differ by some 100 cm^{-1} related to the location of the D atoms. According to the calculations of McCoy and coworkers [3], the lowest energy of the *Cs* (I) configuration was obtained for an arrangement where the three deuterons are placed in the tripod. Schreiner et al. calculated the harmonic zero-point energies of three species for e-*Cs*(I) , s-*Cs*(II) and C_2V structures with amounts of 136.8, 136.4 and132.0 kJ/mol respectively and scaled their harmonic frequencies by 0.95 for estimating an-harmonic effects[16,17]. Although based all five hydrogen atoms possess identical B -H and H-H radial distribution functions within the nuclear vibrational wave function, there is substantial proton scrambling, event 0 K and this is an uncertain result of Keiraninvestigation [15].In addition methane is a quasi-rigid molecule with a well-described molecular structure; however, for its protonation a deep discussion about its electronic structures is needed. This can be related to its abnormal flat potential energy which provides complicated. Large-magnitude motion for taking place which is a reason of fluxionally insists even at a very low temperature ($\neq 0\ K$)due to the QMF or quantum-mechanical fluctuation treatment of the highly correlated from the five protons scrambling motion [16-20].

In 2010 Ivanov and coworkers [21]through of deuterated variants of CH_5^+,exhibited that, in stark contrast to the traditional approach, the Iso-topology spectra of $CH_xD_{(5-x)}^+$ (x=0,1,..5), recorded in an ion trap using the Laser-Induced-Reactions technique, bear almost no resemblance to one another [22, 23]. Through a SCF simulation represents all six vastly different. IR spectra and allow for assigning their aspects. Analysis exactly confirms that the spectra observed for x=1, 2, 3 H and D site occupations are confused but in the x= 4 a breaking of the combinatorial symmetry occurs for those atoms due to QMF within the fluxional molecule [21-23].Via an important procedure, D–H exchange reactions direct to isotope enrichment at low temperatures[5].In 2004, Brown[6] via QDMC has reported the zero point energies for CH_5^+. Due to *Cs* (I) structure described above, the $CD_3H_2^+$variant is of specific interest. Although through hydrogen scrambling approach some of the complexity has been cleared for the quantum ground state of BH_5 and CH_5^+structure, in contrast of quotation in the citation, hydrogen scrambling' is not the root of all the known intricacies. In particular, it has been discussed in this study that CH_5^+undergoes hydrogen scrambling even in the quantum ground state and that the resulting correlated pseudo-rotational dynamics is done by symmetry braking consisting of several small barriers for variants $BH_xD_{(5-x)}$ and $CH_xD_{(5-x)}^+$ [24].

2: Theoretical background

2.1. Electron densities

Electron densities can be explicitly written as e/Bohr^3. $\nabla\rho(r) = [(\frac{\partial\rho(r)}{\partial(x)})^2+(\frac{\partial\rho(r)}{\partial(y)})^2+(\frac{\partial\rho(r)}{\partial(z)})^2]^{\frac{1}{2}}$**(1)** $\nabla^2\rho(r) = \frac{\partial^2\rho(r)}{\partial x^2} + \frac{\partial^2\rho(r)}{\partial y^2} + \frac{\partial^2\rho(r)}{\partial z^2}$**(2)**[25-27].The (-) and (+) values of these functions correspond to the electron densities are locally concentrated and locally depleted respectively. The chemical reactivity, chemical bond type, and electron localization has been built by Bader [28]. We have calculated densities of hydrogen and deuterium in deuterated variants of $BH_xD_{(5-x)}$ via the relationship between $\nabla^2\rho$ and valence shell electron pair repulsion (VSEPR) model [29]**.**

Hamiltonian kinetic energies or K(*r*)cannot be defined individually, since the expected value of kinetic energy operator$<\varphi\ |-\left(\frac{1}{2}\right)\nabla^2|\ \varphi>$**(3)**can be recovered by integrating kinetic energy densities from an alternative definition. One of popular used definition is: $k(r) = -\frac{1}{2}\sum_i \eta_i\varphi_i^*(r)\nabla^2\varphi_i(r)$**(4)**[27-28]. Relative to *K*(*r*), the local definition given below guarantee positives everywhere; hence the physical meaning are clearer and are more generally used [25-27]. The Lagrangian kinetic energies densities, "G(r)" are also known as positive definition as:

$G(r) = \frac{1}{2}\sum_i \eta_i\ |\nabla(\varphi_i|^{\ 2} = \frac{1}{2}\sum_i \eta_i\{[(\frac{\partial\varphi_i(r)}{\partial(x)})^2+(\frac{\partial\varphi_i(r)}{\partial(y)})^2+(\frac{\partial\varphi_i(r)}{\partial(z)})^2]\}$ **(5)**. *G*(**r**) and *K*(**r**) are directly related by Laplacian of electron densities $\frac{1}{4}\nabla^2\rho(r) = G(r) - K(r)$**(6).** By kinetic energy definition via kinetic Monte-Carlo simulations the ground-state zero-point energy from an interpolated PES for estimating the ground-state zero-point energy can be calculated. It has been exhibited that the zero-point energy (ZPE) as a function of the number of distinct data by 150 points has converged to within $\pm$0.5 kJ/mol. According to transition state theory, the frequency with which hydrogen move to the H-H radial distribution function is expressed as: $\Gamma = \vartheta^* \exp(-\frac{\Delta E_h}{K_B T}$**(7)** Where ΔE_h is the difference between the energy at an activated state and the initial equilibrium state, and ϑ^* is an effective vibrational frequency. In this work harmonic approximation of molecular vibrations, isotopes effects on uncoupled vibration is attained through rescaling of the frequency using the reduced masses ration $\omega_D = \omega_H\sqrt{\frac{\mu_H}{\mu_D}}$from the respective Eigen-frequency $\omega_X = \omega_H\sqrt{\frac{K_X}{\mu_X}}$, supposing that the Born–Oppenheimer approximation holds K_D=K_H . Due changing of μ_X for $BHxD_{(5-x)}$(x=0,1,..5),the lagrangian kinetic energy density G(r) and Hamiltonian kinetic energy density K(r) might be different for the deuterated variants (**Fig**.3).

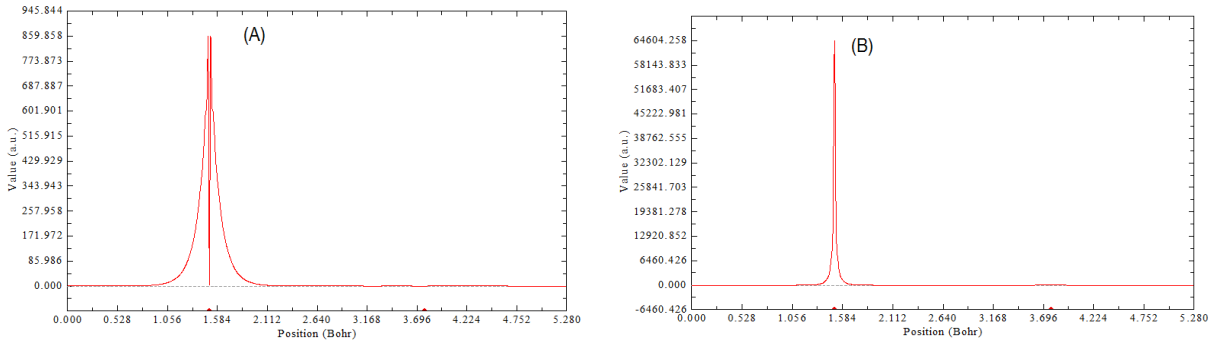

Fig.3: (A): The Lagrangian kinetic energy density G(r) and (B): Hamiltonian kinetic energy density K(r) for the BD_5 .

2.2. Electron localization function

Edgecombe and Beck exhibited spin conditional pair probability has direct correlation with the Fermi hole as a novel electron localization function (ELF) [27]. $ELF(r) = \frac{1}{1+[D(r)/D_{0(r)}]^2}$**(8)** where $D(r) = \frac{1}{2}\sum_i \eta_i \ |\nabla\varphi_i|^2 - \frac{1}{8}[\frac{|\ |\nabla\rho_\alpha|^2}{\rho_\alpha(r)} + \frac{|\ |\nabla\rho_\beta|^2}{\beta(r)}]$**(9)** since $\rho_\alpha(r) = \rho_\beta(r) = \frac{1}{2}\rho$**(10)**, *D* and *D*0 terms can be simplified as $D(r) = \frac{1}{2}\sum_i \eta_i \ |\nabla\varphi_i|^2 - \frac{1}{8}[\frac{|\nabla\rho|^2}{\rho(r)}]$**(11)**,$D_{0(r)} = \frac{3}{10}(3\pi^2)^{\frac{2}{3}}\rho(r)^{\frac{5}{3}}$**(12).**And also for a close-shell system it can be rewrite the equation 9 as: $D_{0(r)} = \frac{3}{10}(6\pi^2)^{\frac{2}{3}}[\rho_\alpha(r)^{\frac{5}{3}} + \rho_\beta(r)^{\frac{5}{3}}]$**(13)**.

Savin *et al*.[30], has reinterpreted ELF in the view of kinetic energy, which makes ELF also useful for Kohn-Sham wave-function in density functional theory. It has been indicated by Tsirelson and Stash [31] that D(**r**) reveals the kinetic energy density caused by Pauli repulsion, while $D_0(\boldsymbol{r})$ can be considered as Thomas-Fermi kinetic energy densities. Localized orbital locator (LOL) is defined and formulized by Schmider and Becke [32] as another novel function for locating high localization regions likewise ELF.$LOL(r) = \frac{\tau(r)}{1+\tau(r)}$**(14)**, and$(r) = \frac{D_0(r)}{\frac{1}{2}\sum_i \eta_i \ |\nabla\varphi_i|^2}$**(15)**, $D_0(r)$for spin-polarized system and close-shell system are defined in the same way as in ELF. In this study the ELF and LOL parameters of hydrogen and deuterium in deuterated variants of $BH_xD_{(5-x)}$and $CH_xD_{(5-x)}^+$ have been calculated for exhibiting the situation and position of five protons scrambling (**Fig**.4).

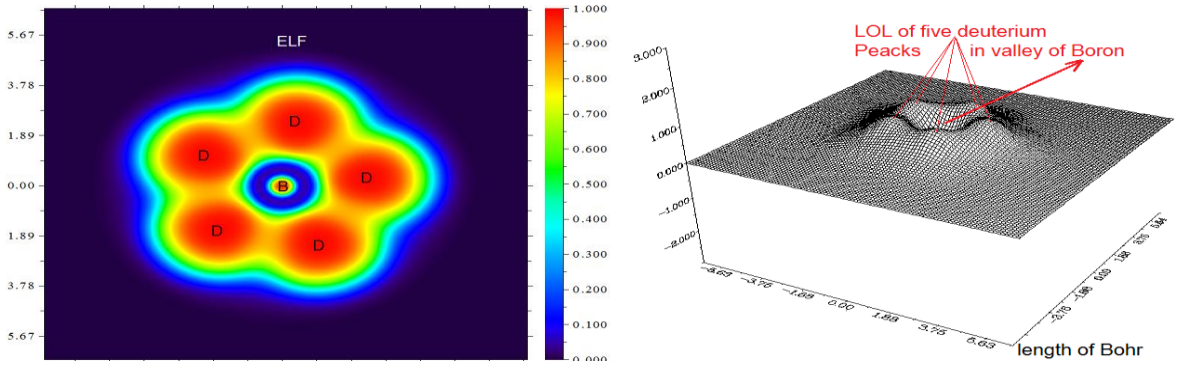

Fig.4: Color filled map of ELF and Relief map of LOL for BD_5

Local information entropies are the quantification of information which firstly was proposed by Shannon in his study about information transmission in noise channel mechanism. Nowadays their applications have been extremely widened to other areas, especially in theoretical chemistry. Many years ago Aslangul and coworkers [33] attempted to decompose diatomic and triatomic molecules into reciprocal monopolized spaces through minimization of information entropies. Parr *et al.* [34] has discussed the relationship among information entropies and atomic partition and

molecular similarities and it has been exhibited the formula of Shannon's information entropies for normalized and continuous probability function is $S = -\int P(x)\ln P(x)dx$ **(16)** while for the chemical systems, if *P*(x) is replaced by$\frac{\rho(r)}{N}$, then the integrand may be called local information entropies of electrons[33]. Through the rearranging the formula it can be shown the $S(r) = -\frac{\rho(r)}{N}\ln\frac{\rho(r)}{N}$**(17)** where, *N* is the total number of electrons in the chemical systems.

2.3. Computational details

Calculations were performed using Gaussian and GAMESS-US packages [35]. In this study we calculate the structures of $BH_xD_{(5-x)}$ and $CH_xD_{(5-x)}^+$ using Moller Plesset, single and double excitations (CISD) and CASSCF(8,9) with an augmented TZ (3d1f1g,2p1d) basis set. The first PES and dipole moment using extensive direct-dynamics of the potential and gradient have been calculated at the CASSCF level of theory with cc-pVDZ and cc-pVTZ basis sets[36].Through redundant internal coordinates, several PESs in few inter-nuclear distances have been fit to these data. The potential energies and gradient data for each atoms of $BH_xD_{(5-x)}$ and $C_HxD_{(5-x)}^+$generated analytical multinomial expression, using Multi-wfn analyzing software[27]as variables the complete set of inverseinter-nuclear distances. The Perdue-Burke-Ernzerhof [37](PBE)exchange-correlation (XC) functional of the generalized gradient approximation (GGA) is adopted. Based our previous works concerning the approaches of ELF, LOL and density quantum energies, we strive to discuss a useful method for understanding more about $CH_xD_{(5-x)}^+$ treatments[38-50].

3. Results and discussions

3.1. Potential energy surfaces

The fitted potential energy surfaces are tested by comparing it against additional electronic energy calculations and by comparing normal mode frequencies at the three lowest-lying stationary points obtained from the fitting against ab-initio ones. Rotational constants along the B-H and B-D bond lengths and the tunneling coordinates via ELF, LOL, energy densities, Local information entropy , geometry optimization of variant $BH_xD_{(5-x)}$(X=0 to 5) and related normal modes have been calculated and are presented in **Table**s 1-5 and **Fig**ures 1-9.

Table1. Energy densities, ELF, LOL, and local information for BD_5viaccsd(T)/AUG-cc-pvdz

Atoms	B-D Bond length	Electron density	ESP from electron (10^2)	Lagrangian kinetic [G(r)]	Hamiltonian kinetic [K(r)]	Potential energy Density [U(r)]	Electron localization function (ELF)	Local information entropy	Average local ionization energy	Eta index	Localized orbital locator (LOL)
B(1)	-	0.678	-0.136	0.149	0.646	-0.646	0.99	-0.129	0.737	-1.00	0.994
D(2)	1.206	0.260	-0.429	0.185	0.225	-0.227	0.99	0.949	0.679	-1.05	0.949
D(3)	1.201	0.260	-0.429	0.185	0.225	-0.227	0.99	0.946	0.678	-1.04	0.949
D(5)	1.205	0.260	-0.428	0.186	0.224	-0.228	0.99	0.948	0.679	-1.04	0.942
D(4)	1.204	0.260	-0.425	0.185	0.225	-0.228	0.99	0.949	0.679	-1.06	0.941
D(6)	1.203	0.261	-0.426	0.184	0.224	-0.227	0.99	0.949	0.679	-1.07	0.940

In addition they have compared with the corresponding harmonic oscillator and standard classical molecular dynamics data. The delocalization of the wave function is analyzed through the Multiwfn software [25-27] comparison of the BX_5(X=H and D) distributions with those obtained when all of the hydrogen atoms are replaced by deuterium. The

data of density energies, charges from ESP, electrostatic potential, ionization energy, ellipticity of electron densities, and Eta index for boron, deuterium and hydrogen are listed in **Table**s [1-3],and **Fig**ures 5&6. The data are indicated of five equal situations in boron-hydrogen bonds

Table.2: Energy densities, ELF, LOL, and local information for BH5 with CASSCF(8, 9)/cc-pvdz, quantum calculations.

Atoms	B-H bond length	Electron density	Lagrangian kinetic [G(r)]	Hamiltonian kinetic [K(r)]	Potential energy Density [U(r)]	Electron localization function (ELF)	Local information entropy	Average local ionization energy	Eta index	Localized orbital locator (LOL)
H(2)	1.185	0.259	0.183	0.222	-0.227	0.991	0.941	0.671	-1.04	0.951
H(3)	1.182	0.261	0.181	0.223	-0.224	0.993	0.944	0.670	-1.01	0.950
H(5)	1.183	0.263	0.182	0.224	-0.223	0.992	0.941	0.672	-1.03	0.949
H(4)	1.181	0.264	0.184	0.223	-0.225	0.992	0.945	0.673	-1.02	0.948
H(6)	1.181	0.261	0.185	0.222	-0.221	0.991	0.943	0.670	-1.05	0.949

Table3.ESP, Energy densities and LOL information for H atoms in variants $BH_xD_{(5-x)}$

Hydrogen properties inBHxD(5-x)	ESP (10^2)	Lagrangian kinetic [G(r)]	Hamiltonian kinetic [K(r)]	Potential energy Density [U(r)]	Electron localization function (ELF)	Local information entropy	Average local ionization energy	Eta index	Localized orbital locator (LOL)
BHD_4 :x=H(6)	-0.423	0.180	0.221	-0.220	0.993	0.944	0.671	-1.05	0.942
$BH2D_3$:x=H(6)	-0.421	0.182	0.222	-0.221	0.994	0.945	0.673	-1.04	0.944
$BH2D_3$:x=H(4)	-0.425	0.181	0.222	-0.220	0.991	0.944	0.674	-1.03	0.949
$BH3D_2$:x=H(4)	-0.424	0.183	0.219	-0.223	0.993	0.940	0.675	-1.03	0.949
$BH3D_2$:x=H(5)	-0.427	0.181	0.220	-0.222	0.994	0.943	0.673	-1.06	0.950
BH4D :x=H(2)	-0.423	0.179	0.220	-0.221	0.992	0.942	0.672	-1.04	0.947
BH4D :x=H(3)	-0.425	0.180	0.221	-0.221	0.991	0.941	0.671	-1.05	0.948
BH5:x=H(4)	-0.426	0.184	0.223	-0.225	0.992	0.945	0.673	-1.02	0.948
BH5 :x=H(6)	-0.427	0.185	0.222	-0.221	0.991	0.943	0.670	-1.05	0.949

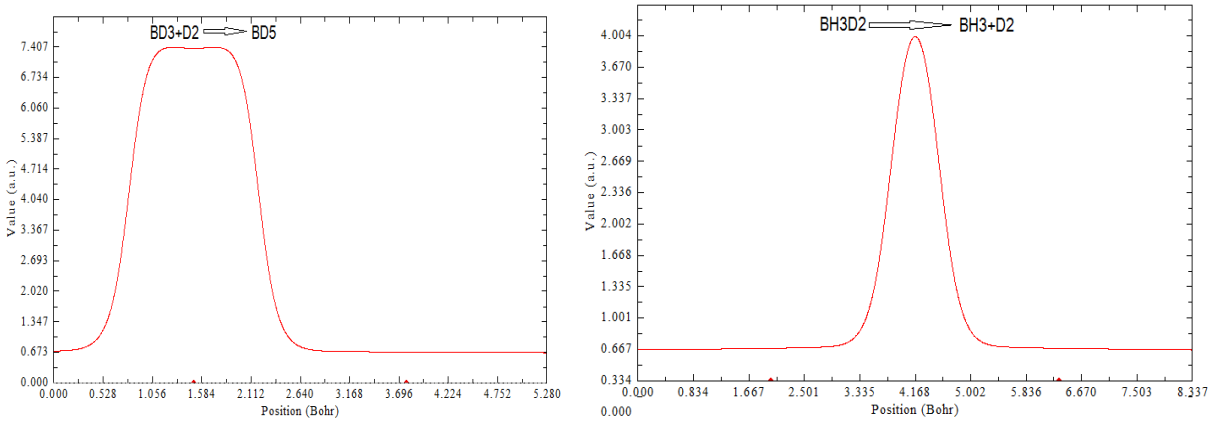

Fig.5: Average local ionization energy for $BD_5$and BH3D2 in two position of 1.584 and 4.168 Bohr respectively

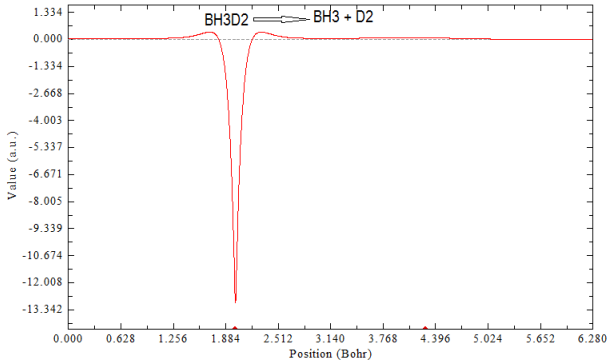

Fig.6: Local information entropy indicate the mechanism of dissociation of BH3D2 to BH3 and D2

3.2. Elf and LOL Mechanism

ELF has been calculated via the equation 8 and as well as LOL has been done through equations 14, 15.The variant densities for open and closed-shell systems have been estimated via equations 9-13. The spin density from the difference between alpha and beta densities can be calculated through the expression of $\rho^s(r) = \rho^\alpha(r) - \rho^\beta(r)$, then the spin polarization parameter function returned instead of spin density $\xi(r)=\frac{\rho^\alpha(r)-\rho^\beta(r)}{\rho^\alpha(r)+\rho^\beta(r)}$.If electrons are completely localized, then they can be distinguished from those outside. Bader[26] found that the areas which have large electron localization might have large magnitudes of Fermi whole integration. Although*D*0(**r**) from Eqs 11–13 is introduced into ELF as a reference, the ELF reveals basically a relative localization (ELF is within the range of [0, 1]). A large ELF values means that electrons are extremely localized, which indicates that there are covalent bonds in the regions. Based on ELF variables (as it can be seen in the **Table**s1-4), all X-B strength bonds are equal with strong covalent bonds. As a result, the mechanism disassociation of the $BH_xD_{(5-x)}$to produceH_2 or D_2seems bizarre but is true. Ivanov and coworkers [21] have discussed through assigning the spectra of the isotopologues with experimental and computed IR spectra of CH_5^+ and all its H/D isotopologues(including mass-rescaled CD_5^+ and CH_5^+)with the simulated spectra to a particular mode (except for bends).Based on full decomposition intoisotopomer contributions, they exhibited subsequent spectral disentangling proton occupation probabilities in the moiety where upper/lower bars indicate the quantum/classical distributions. It has been believed that within classical mechanics, the five different sites in the BX_5 like CX_5^+ are expected to be populated by H or D for all category of $B_HxD_{(5-x)}$and also $CH_xD_{(5-x)}^+$. Based on our results, it is supposed that only two bonds of B-X in a part of molecules exhibit properly quantum effects on the nuclei (as quantum particles through the high rotation) while remain parts of the molecules have classical particle behavior (lower rotation)which is so-called art factual rotational motion.ELF has been widely used for wide variety of systems, such these kind of small molecules for revealing the atomic shell structure and the classification of chemical bonding to verify charge-shift bonds. This approach became stronger via LOL data which has similar expression compared to ELF. Jacobsen pointed out that LOL conveys more decisive and clearer picture than ELF; obviously LOL can be interpreted in kinetic energy in the same way as for ELF; however LOL can also be interpreted in point view of localized orbital. Small (large) LOL values usually appear in the boundary (inner) area of localized orbital's because the gradient of the orbital wave-function is large (small) in this area. The value range of LOL is identical to ELF, namely [0, 1] and the data are listed in **Table**s 4 and are plotted in **Fig** 7

Table4.ESP, Energy densities and LOL information for B atoms for variants $BH_xD_{(5-x)}$

Carbon properties in $BH_xD_{(5-x)}$	ESP (10^2)	Lagrangian kinetic [G(r)]	Hamiltonian kinetic [K(r)]	Potential energy Density [U(r)]	Electron localization function (ELF)	Local information entropy	Localized orbital locator (LOL)
BH5	-0.136	0.149	0.649	-0.646	0.998	-0.129	0.991
BHD_4	-0.135	0.148	0.650	-0.649	0.991	-0.128	0.992
$BH2D_3$	-0.134	0.147	0.651	-0.650	0.992	-0.125	0.993
$BH3D_2$	-0.133	0.146	0.652	-0.651	0.993	-0.126	0.991
BH4D	-0.132	0.145	0.653	-0.652	0.991	-0.127	0.992

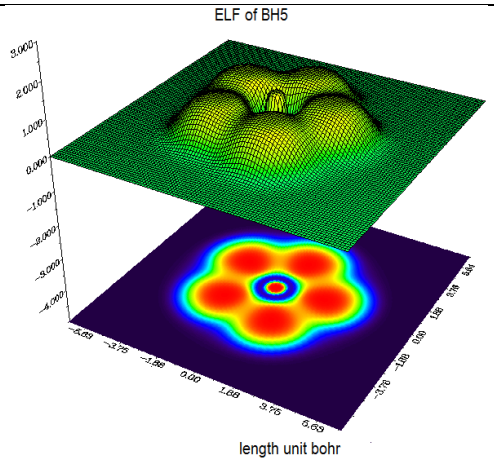

Fig.7.ELF Shaded surface map with projection of BH5

3.3. Normal mode analyzing

Normal mode analyzing has been exhibited protons are prefer to accumulate in the X_2 moiety for all mixed isotopologues whereas deuterons prefer to be in the BX_3 tripod based on quantum approaches(**Table**s5-7 and **Fig**s 8&9). Average local ionizations for separated fragments are shown in **Fig**.5&6that indicates the energy separation is a function of HD situation, which are equal for $BH_5 \rightarrow BH_3+H_2$ or $BH3D2 \rightarrow BH_3+D_2$.The B(1)-H(6) stretching band as a lowest-frequency has been associated with the relative motion of the H_2 moiety with respect to the methyl tripod in Prorogated methane which indicates that BH5 is actually composed of those two subunits, BX_3 and X_2in the hydrogen scrambling. Energy level diagram (**Fig**.5&6 and **Table** 5) shows the two energetically accessible dissociation limits of BH_5, which is formed with Cs on the neutral surface. The results of ellipticity of electron density from **Table**s1-4 described using the correct "fluxional" phase-spaces sampling of BH5 which are vertical, resonant, and non-resonant in good corresponding with the experimental data. This channel exhibits a bimodal distribution that the explanation for this shoulder comes from consideration of the HH, HD and DD bond lengths distribution in the parent $BH_xD_{(5-x)}$and the portion of that distribution correlates with BX_3+ X_2productsmore significantly which are shown in **Fig**s4-6.Ivanov [21] and coworkers have shown that classical ab initio molecular dynamics indeed reproduces closely the binomial distributions expected for those site occupations while the full quantum simulations reveal the quantum populations strongly deviating from classical (binomial) occupations. Here, there is a point; is there any real or art factual rotational motion in quantum approaches? In other words, there is a symmetry breaking among classical towards quantum approaches only for X_2 as a part of molecule. On partial $D \leftrightarrow H$ substitutions, scrambling phenomenon

appeared in different isotopic nuclei for populating all available sites, that is, those in the X_2 moiety. The local information entropy data in **Table**s1-4 and entropy in **Table**.6indicate that $BH_xD_{(5-x)}$ is binomial distributions but for two parts inside the molecule. Considering the differences in zero-point energies of D and H, it might be indicated that deuterons prefer to populate the BX_3 tripod in the mixed isotopologuesBH_4D and BHD_4, whereas protons conjecture in the X_2 moiety are compared to the purely combinatory probabilities. Quantum-mechanical fluctuations due to Boltzmann statistics cause systematic deviations of the H and D sites from the underlying combinatorial symmetries, and thereby induce a breaking of that symmetry. The Localized orbital locator and electron localization function (**Table**1-4) have confirmed the approaches of quantum localization in this work. This effect is relevant at all for the vibrational normal modes and as it can be seen, these intricate nuclear quantum effects are certain ways for understanding the experimental spectra[54]. Distribution correlating with BH_3 and $CH_3^+$and H_2 exhibits a larger contribution with the shorter one of H-H distance than the longer one. In addition, vibrational excited state of H-H with the larger hydrogen-hydrogen bond length indicates a greater contribution than the shorter one (in contrast D-D), while for H-Admit depends to isotopologues combinations. Through the normal modes analysis (**Table**s 5-7 and **Fig**.8), it can be seen that partial $D \leftrightarrow H$ substitutions break the rotational symmetry.

Table5. Rotational temperatures, Rotational constants, Zero-point vibrational and E (Thermal) for variants of $B_HxD_{(5-x)}$ and $C_HxD_{(5-x)}^+$

$BH_xD_{(5-x)}$	Molecular mass amu	Diagonal vibrational polarizability x y z			Rotational constants (GHZ)			Zero-point vibrational Energy(Kcal/Mol)	E (Thermal) (Kcal/Mol)
BD5	21.079	22.82	22.59	89.24	68.97	68.91	34.47	55.61	57.73
BHD_4	20.073	23.18	22.73	89.43	89.84	70.98	39.65	60.38	62.48
$BH2D_3$	19.067	23.23	22.8	89.5	99.93	82.31	45.13	64.86	66.92
$BH3D_2$	18.060	23.08	23.08	89.62	111.18	96.86	51.76	69.31	71.35
BH4D	17.054	22.90	22.91	89.44	141.71	103.16	59.71	73.69	75.71
BH5	16.048	22.85	22.59	89.24	141.98	141.74	70.93	77.81	79.79
$CH_xD_{(5-x)}^+$	Molecular mass amu	Rotational Temperatures x y z total				Rotational constants (GHZ)			Zero-point vibrational Energy(Kcal/Mol)	E (Thermal) (Kcal/Mol)
$CD5^+$	22.070	3.135 2.607		2.749	4.92	65.327	57.293	54.339	23.643	25.997
CHD_4^+	21.064	3.345 3.010		3.013	5.42	69.699 62.737		62.781	25.244	27.538
$CH2D_3^+$	20.057	3.886 3.147		3.625	6.18	80.982	75.540	65.581	27.063	29.318
$CH3D_2^+$	19.051	4.496 3.562		4.151	7.09	93.693 74.237		86.494	28.620	30.825
$CH4D^+$	18.045	5.480	4.554	4.227	8.29	114.199	94.906	88.081	30.528	32.705
$CH5^+$	17.039	6.258 4.562		4.818	9.11	130.40 95.05		100.392	31.744	33.811

Table6. Zero-point and Sum of electronic energies, C_V and entropy for variants of $BH_xD_{(5-x)}$ and $C_HxD_{(5-x)}^+$

BHxD(5-x)	**Sum of electronic and zero-point Energies**	**Sum of electronic and thermal Energies**	**Sum of electronic and thermal Enthalpies)**	**Sum of electronic and thermal Free Energies**	**C_V& S Cal/Mol-Kelvin**
BD5	-27.404427	-27.401042	-27.400098	-27.426176	8.812 54.88
BHD4	-27.396812	-27.393472	-27.392527	-27.418300	8.68154.244
BH2D3	-27.389684	-27.386391	-27.385447	-27.410888	8.53453.547
BH3D2	-27.382594	-27.379346	-27.378401	-27.403503	8.38852.831
BH4D	-27.375606	-27.372398	-27.371454	-27.396200	8.2352.08
BH5	-27.369047	-27.365881	-27.364937	-27.389302	8.0851.28
CHxD(5-x) +	**Sum of electronic and zero-point Energies**	**Sum of electronic and thermal Energies**	**Sum of electronic and thermal Enthalpies)**	**Sum of electronic and thermal Free Energies**	**C_V& S Cal/Mol-Kelvin**
CD5+	-40.564275	-40.560524	-40.559579	-40.586386	10.662 56.419
CHD4+	-40.561723	-40.558069	-40.557125	-40.583540	10.229 55.596
CH2D3+	-40.558824	-40.555232	-40.554288	-40.580354	9.822 54.860
CH3D2+	-40.556343	-40.552831	-40.551886	-40.577516	9.548 53.941
CH4D+	-40.553303	-40.549834	-40.548890	-40.574168	9.211 53.201
CH5+	-40.544916	-40.541623	-40.540679	-40.565387	8.914, 52.00

Table7. Normal modes Vibration temperatures for variants $BH_xD_{(5-x)}$

Normal modes Vibration temperatures	(1)	(2)	(3)	(4)	(5)	(6)	(7)	(8)	(9)	(10)	(11)	(12)
BD5	839.0	838.4	473.8	437.6	439.3	1700.9	1937.3	1937.5	2205.3	2205.9	13993.8	14042.7
BHD4	985.0	839.0	490.7	441.7	487.0	1744.5	1937.6	2067.9	2205.7	2759.3	14029.9	16569.1
BH2D3	1093.1	868.3	516.9	470.6	517.1	1819.3	1979.8	2123.4	2736.1	2784.1	14540.8	18400.4
BH3D2	1161.1	938.4	540.1	514.1	532.9	1909.9	2005.5	2642.3	2771.1	2840.6	15848.0	19419.1
BH4D	1185.1	1055.8	558.3	525.8	584.1	1949.2	2519.9	2738.7	2818.2	2869.0	17724.2	19822.0
BH5	1186.08	1185.2	584.5	586.7	588.9	2404.6	2738.7	2739.02	2868.7	2869.1	19782.7	19851.8

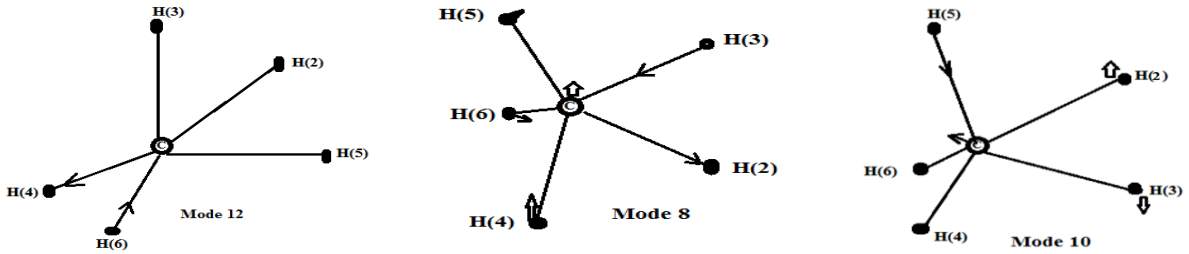

Fig.8. Frequencies 10,8,12 Modes of vibrations

4. Conclusion

The spectrum of mode 12 is highly complex with huge red-shifts and some blue-shifts. In particular, they can be attributed to the rapid coupling of the original BH-stretching normal mode to motions more closely related to isomerization, i.e., bending or rocking. There has thus been a long debate whether BH_5 has a structure at all or not and it has real or art factual structure. It is supposed that only two bonds of B-X in a part of molecules obey quantum populations while remain parts of the molecules have a classical occupations which there is an art factual structure.

References:

[1] D. Marx, M. Parrinello, *Science*. , 284(1999), 59.

[2] P. R. Schreiner, *Angew. Chem. Int. Ed*. ,39, 18 (2000), 3239.

[3]A. B. McCoy, B. J. Braams, A. Brown, X. Huang, Z. Jin , J. M. Bowman, *J. Phys. Chem.*, A, 108, (2004), 4991.

[4] A. L. Kaledin, S. D. Kunikeev, H. S. Taylor, *J. Phys. Chem. A.*, 108, (2004), 4995.

[5] A. Brown, B. J. Braams, K. Christoffel, Z. Jin, J. M. Bowman, *J. Chem. Phys.*,119, (2003), 8790

[6] A. Brown, A. B. McCoy, B. J. Braams, Z. Jin, J. M. Bowman, *J. Chem. Phys*., 121, (2004), 4105.

[7] G.A. Olah, G. Rasul, F. Kekule, *Acc. Chem. Res*., 30, (1997), 245–250.

[8] M. M. Kreevoy, J.E.C. Hutchins, *J.Am.Chem.Soc*.94, (1972), 6371.

[9] J.B.Collins, P.V.R.Schleyer, J.S.Binkley, J.A.Pople, *J.Am.Chem.Soc*.98, (1976), 3438.

[10]G.A. Olah, G.K.S.Prakash, R.E. Williams, L.D. Field, K. Wade,*Hypercarbon Chemistry* Ch. 1, 5, 7 (Wiley, 1987).

[11] T. Oka, *Phil. Trans. R. Soc. Lond. A* 324, (1988) 81–95.

[12] E.Herbst, *J. Phys. Chem. A.*, 109, (2005) 4017–4029.

[13]D. Gerlich, *Phys. Chem. Chem. Phys*. 7, (2005), 1583–1591.

[14] H.H. Micheles, F.F. Harris, J.B. Addison, *International Journal of Quantum chemistry*. 4, (1971) 149-151.

[15] C.Keiran, T. Deborah,L.Crittenden, J. Meredith, T. Jordan,*J. AM. CHEM. SOC*. 127, (2005), 4954-4958.

[16] P.R. Schreiner, S.J. Kim, H.F. Schaefer, P.V.R.Schleyer, *J. Chem.Phys*. 99, (1993), 3716.

[17]V. Dyczmons, W.Kutzelnigg, *Theoret. Chim.Acta (Berlin)* 33, (1974) 239–247.

[18]H. Muller, W.Kutzelnigg, J.Noga, W.Klopper, *J. Chem. Phys*. 106, (1997),1863–1869.

[19]D. Marx, M.Parrinello, *Nature* 375, (1995), 216–218.

[20] P.R.Schreiner, H.F. Schaefe, P.V.R.Schleyer , *The Journal of Chemical Physics*.,01(9), (1994)7625-7632.

[21] S. D. Ivanov, O. Asvany, A.Witt, E. Hugo, G. Mathias, B. Redlich, D. Marx,S.Schlemmer,*Nature Chemistry*, (2010) , 298–302.

[22] S. Schlemmer, E.Lescop, J.Richthofen, D.Gerlich, M. Smith, *J. Chem. Phys*. 117, (2002) 2068–2075.

[23]. S. Schlemmer, O.Asvany, *J. Phys.: Conf. Series* 4, (2005),134–141.

[24] A. J. R. Heck, L. J. de Koning, N. M. M. Nibbering, *J. Am. Soc*., 2,(1991), 453.

[25] T. Lu, F.Chen,*ActaChim. Sinica.*, 69, (2011),2393-2406.
[26] T. Lu, F. Chen, *J. Mol. Graph. Model* 38, (2012) 314-323.
[27]T. Lu, F. Chen, *J. Comp. Chem.*, 33, (2012) 580-592.
[28] R.F.W. Bader, *Oxford Univ. press, Oxford*, (1990).
[29] Becke and Edgecombe*J. Chem. Phys*., 92, (1990), 5397.
[30]Savin et al *Angew. Chem. Int. Ed.Engl*., 31, (1992), 187.
[31] Tsirelson and Stash, *Chem. Phys. Lett.*, 351, (2002), 142.
[32]Schmider and Becke, *J. Mol. Struct., (THEOCHEM)*, 527, (2000), 51.
[33]Aslangul and coworkers, *Adv. Quantum Chem.*, 6, (1972), 93.
[34]Parr et al, *J. Phys. Chem. A*, 109,(2005), 3957.
[35] M.W.Schmidt, K.K.Baldridge, J.A.Boatz, S.T.Elbert, M.S.Gordon, J.H.Jensen, S.Koseki, N.Matsunaga, K.A.Nguyen 14(11) (2004)1347–1363.
[36]T. H. Dunning, *J. Chem. Phys*. 90,(1989), 1007.
[37] J.P. Perdew, K.Burke ,Ernzerhof, *Phys. Rev. Lett.* 77, (1996) 3865-3868.
[38] M. Monajjemi, J.E. Boggs, *J. Phys. Chem. A***,**117,(2013) 1670 −1684.
[39]M. Monajjemi, V.S. Lee, M. Khaleghian, B. Honarparvar, and F. Mollaamin, *J. Phys. Chem. C*. 114 (2010) 15315.
[40] M. Monajjemi. *Journal of Molecular Modeling* ,20, (2014), 2507.
[41] M. Monajjemi,*Theor Chem Acc*,134,(2015)77.
[42] M. Monajjemi, *Struct. Chem*, 23,(2012) 551.
[43] M. Monajjemi,*ChemicalPhysics*.425, (2013) 29-45.
[44] H. Jalilian, M. Monajjemi, *Japanese Journal of Applied Physics*.54, (2015) ,085101.
[45] M. Monajjemi, M. Khaleghian, *Journal of Cluster Science*.22(4) (2011), 673-692.
[46] M. Monajjemi, M. Falahati, F. Mollaamin, *Ionics*,19, 1,(2013),155-164.
[47] M.Monajjemi, *Biophysical Chemistry*. 207,(2015)114 –127.
[48]L**.** Mahdavian, M. Monajjemi, *Microelectronics Journal*. 41(2-3), (2010), 142-149.
[49] M. Monajjemi, *Journal of Molecular Liquids*,230**,**(2017), 461-472.
[50]M. Monajjemi**,** *Macedonian Journal of Chemistry and Chemical Engineering*, 36, 1, (2017) 101–118.